JOURNAL OF GEOPHYSICAL RESEARCH, VOL. 94, NO. A6, PAGES 6995–7001, JUNE 1, 1989

# Electron Velocity Distributions and Plasma Waves Associated With the Injection of an Electron Beam Into the Ionosphere

L. A. FRANK,[1] W. R. PATERSON,[1] M. ASHOUR-ABDALLA,[2,3] D. SCHRIVER,[3,4]
W. S. KURTH,[1] D. A. GURNETT,[1] N. OMIDI,[3] P. M. BANKS,[5]
R. I. BUSH,[5] AND W. J. RAITT[6]

An electron beam was injected into Earth's ionosphere on August 1, 1985, during the flight of the space shuttle *Challenger* as part of the objectives of the Spacelab 2 mission. In the wake of the space shuttle a magnetically aligned sheet of electrons returning from the direction of propagation of the beam was detected with the free-flying Plasma Diagnostics Package. The thickness of this sheet of returning electrons was about 20 m. Large intensifications of broadband electrostatic noise were also observed within this sheet of electrons. A numerical simulation of the interaction of the electron beam with the ambient ionospheric plasmas is employed to show that the electron beam excites electron plasma oscillations and that it is possible for the ion acoustic instability to provide a returning flux of hot electrons by means of quasi-linear diffusion.

## INTRODUCTION

Spacelab 2 was carried into an orbit with altitude ~320 km and inclination 49.5° on the space shuttle *Challenger* on July 29, 1985. During August 1 the Plasma Diagnostics Package (PDP) was put into free flight around *Challenger* in order to measure phenomena associated with the passage of a large vehicle through the ionosphere, the injection of electron beams, the release of volatiles, and the ambient ionosphere. The PDP provided observations out to a distance of ~400 m from the space shuttle before it was retrieved on the same day. A Langmuir probe, an ion mass spectrometer, a hot plasma analyzer, a differential ion flux probe, and a plasma wave receiver were among the instruments on board the PDP. For a description of this instrumentation the reader is referred to *Shawhan* [1982]. Of relevance to the present investigation are the measurements of the three-dimensional velocity distributions of electrons in the energy range 2 eV to 36 keV with the hot plasma analyzer, the LEPEDEA, and of the spectral energy density of the electric fields of plasma waves in the frequency range from 31 Hz to 17.8 MHz. These two instruments were used to observe the electrons and plasma waves produced by the 1-keV electron beam injected into the ionosphere with the fast pulse electron generator (FPEG) that was located in the bay of the shuttle. The implementation of the FPEG was the joint responsibility of Stanford University and Utah State University [see *Raitt et al.*, 1982], and the PDP was designed and constructed at The University of Iowa. We present initial observations of hot electrons and plasma waves that are produced by the electron beam. The effects are confined to a narrow, magnetically aligned sheet in the wake of the shuttle. The results of a numerical simulation are used in order to interpret the large intensities of hot electrons that return from the direction of beam injection and the presence of intense broadband electrostatic noise.

The first artificial injection of an electron beam into the ionosphere was reported by *Hess et al.* [1971]. Even for this early experiment it was noted that the ambient electron plasmas were heated by the electron beam. The early rocket-borne experiments were primarily focused on exciting artificial auroras and providing a means for investigating the motion of electrons between their geomagnetic mirror points. More recently, the scientific thrust has been directed toward understanding the heating of electron plasmas and the generation of plasma waves by the electron beam because of the relevance of these phenomena to mechanisms for the interaction of the naturally occurring auroral electron beams with the ionosphere. The artificial electron beams offer a unique opportunity to determine the beam-plasma interactions that can heat ionospheric electron plasmas greatly in excess of that expected from direct Coulomb interactions [cf. *Maehlum et al.*, 1980, and references therein]. An extensive review of early experiments with artificial electron beams is given by *Winckler* [1980].

Previous injections of an artificial electron beam from the space shuttle were accomplished during the STS 3 and Spacelab 1 missions. During the Spacelab 1 mission a large flux of returning hot electrons was observed [*Wilhelm et al.*, 1984], and whistler mode, narrow-band emissions near $3f_c$ and $4f_c$ ($f_c$, electron cyclotron frequency) and broadband electrostatic noise were clearly present [*Beghin et al.*, 1984]. These plasma and plasma wave measurements were obtained in the bay of the space shuttle. The instrumentation used for the STS 3 mission was similar to that for the Spacelab 2 mission, except that the PDP was not released into free flight from the space shuttle. Observations of electromagnetic radiation during the electron beam firings of the STS 3 mission are reported by *Reeves et al.* [1988*a*]. *Winglee and Pritchett* [1988] give the results of a numerical simulation model to account for the complex behavior of the electron beam in the immediate vicinity of the electron gun nozzle when the beam electrons are expected to execute a coherent helical motion about the local magnetic field. The

[1]Department of Physics and Astronomy, University of Iowa, Iowa City.
[2]Department of Physics, University of California, Los Angeles.
[3]Institute of Geophysics and Planetary Physics, University of California, Los Angeles.
[4]Now at Max-Planck Institute for Extraterrestrial Physics, Garching, Federal Republic of Germany.
[5]STAR Laboratory, Stanford University, Stanford, California.
[6]Center for Atmospheric and Space Sciences, Utah State University, Logan.



Paper number 89JA00507.
0148-0227/89/89JA-00507$02.00

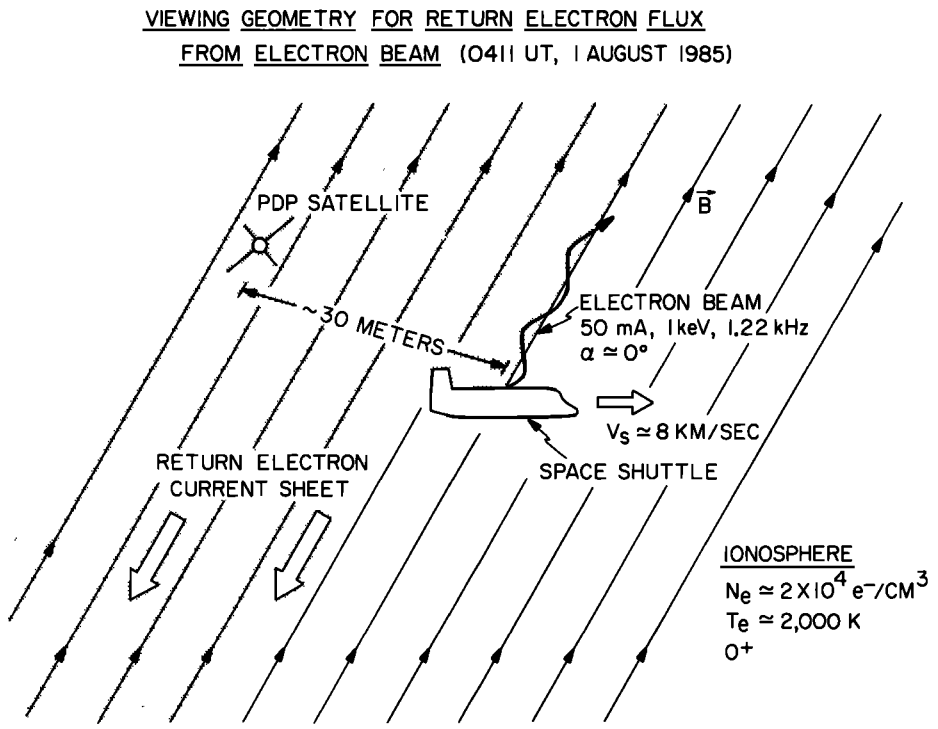


Fig. 1. Viewing geometry for observing the electron velocity distributions and plasma waves produced by the launching of an electron beam from the bay of the space shuttle *Challenger*.

beam density is large in relation to the ambient ionospheric density, and the beam is expected to lose its coherency, i.e., its collimated spiral motion along the ambient magnetic field, within scale lengths of meters from the injection point. This simulation was not carried forward in time sufficiently long to identify the presence of low-frequency ion waves. Our present study uses observations of the effects of the beam electrons at much larger distances from the space shuttle during the Spacelab 2 mission, i.e., the escaping electrons, and a numerical simulation that reveals the probable generation of ion acoustic waves. Our presently reported observations were taken with instruments on board the PDP during its several-hour free flight around the space shuttle and hence are relatively uncompromised by shuttle-associated effects. These unique observations of electron plasmas and plasma waves provide the basis for a significant extension of knowledge of electron beam-plasma interactions.

## Observations

The PDP encountered the sheet of returning electrons during eight FPEG beam launching sequences. Our presentation concentrates on the sequence that occurred for 430 s beginning at 0411:13 UT. The situation is depicted in Figure 1. The 1-keV electron beam was modulated at a 1.22-kHz frequency with a 50% duty cycle. The current was 50 mA. Inspection of observations when the beam was unmodulated shows that the modulation of the current has no apparent effect on the phenomena reported here. During the period 0411:13–0412:02 UT a large flux of hot electrons was encountered. The velocity distribution function is anisotropic with measurable densities at all pitch angles and with maximum densities corresponding to fluxes returning to the ionosphere. The injected electron beam was propagating away from the ionosphere. The thickness of this field-aligned current sheet was about 20 m as measured for several crossings during operation of the FPEG. For comparison the gyroradius of a 1-keV electron moving perpendicular to the local magnetic field vector is 4.9 m. For the measurements of electrons presented here, the electron beam is injected nearly parallel to the magnetic field. During the above time period the PDP moved from a position ~15 m downstream from field lines intersecting the shuttle to ~45 m as it crossed out of the current sheet. During another electron beam injection this electron sheet was seen to extend at least to 170 m behind the shuttle. Such field-aligned electron distributions were not observed when the PDP was positioned outside the expected location of the sheet when the electron gun was activated. The velocity distribution of hot electrons returning along the magnetic field ($\alpha \simeq 165°$) at 0411:26 UT is shown in Figure 2. The anisotropy is large. For electrons with pitch angle $\alpha \simeq 15°$, $f \simeq 10^{-28}$ s$^3$/cm$^6$ at $v = 6 \times 10^8$ cm/s, i.e., a factor of ~100 less than that of the returning electron flux at $\alpha \simeq 165°$. The phase space density increases with decreasing electron speed, and the electron number density integrated over all pitch angles is ~100 el/cm$^3$ for $E \gtrsim 2$ eV. The energy spectrum and angular distributions are qualitatively similar to those observed previously during beam injections into the ionosphere from rockets [*Winckler et al.*, 1975; *Duprat et al.*, 1983; *Wilhelm et al.*, 1985]. The upper limit for the electron velocity distribution at similar pitch angles but just outside the sheet while the FPEG was still activated at 0412:19 UT is also shown in Figure 2.

The possibility that the returning electrons are due to backscattering from the ambient neutral atmosphere must be evaluated in order to identify the current sheet as a signature of a beam-plasma interaction. We have numerically esti-

mated the contribution from atmospheric scattering using the relationship

$$\frac{d^2j_s}{dEd\Omega} = j\rho \frac{d^2\sigma}{dEd\Omega} \frac{Vt \sin \alpha}{(V \cos \alpha/V_b - 1)^2} \quad (1)$$

where $j_s$ is the secondary flux, $V$ is the speed of these electrons, $\alpha$ is their pitch angle, $V_b$ is the speed of the beam electrons, $j$ is the beam directional flux, and $\rho$ is the atmospheric number density. The mass spectrometer incoherent scatter 1983 (MSIS-83) model [*Hedin*, 1983] is used for atmospheric densities. The differential cross section $d^2\sigma/dEd\Omega$ is approximated using the laboratory measurements reported by *Opal et al.* [1971] for several gases, but not atomic oxygen. The total scattering cross section for O I was taken to be one-half that given for $O_2$. It should be noted by the reader that the electron gun is moving with respect to the ambient atmospheric molecules and that numerical integration of equation (1) must include the condition of appropriate combinations of $V$, $\alpha$, and $t$ in order that the secondary electron from a given distance from the shuttle reaches the PDP at energy $E$. Then the time $t$ is the elapsed time since the injection of the beam electron. The electron beam is injected at an altitude of ~320 km and in the direction away from the atmosphere. Further scattering of the secondary electrons before arrival at the PDP is neglected in these calculations. For the purpose of this estimate the primary electron beam is assumed to be monoenergetic, 1 keV, with no significant energy and pitch angle diffusion due to beam-plasma interactions. The computed field-aligned intensities of electrons from atmospheric scattering are shown in Figure 2. Open circles indicate the energies at which equation (1) was evaluated. At low energies these intensities are lower than the observed intensities by factors of ~100. Confidence in the calculated scattered intensities is supported by reasonable agreement of these intensities with those observed further downstream in the electron sheet where the electron intensities may be expected to be due mainly to atmospheric scattering. No evidence was found in the LEPEDEA ion measurements for significant increases of thermal or suprathermal ion densities that are expected to occur from ionization of the ambient neutral atmosphere by a beam-plasma discharge (see *Grandal* [1982] for discussions of this phenomenon). Thus the field-aligned intensities reported here are likely to be due to a beam-plasma interaction.

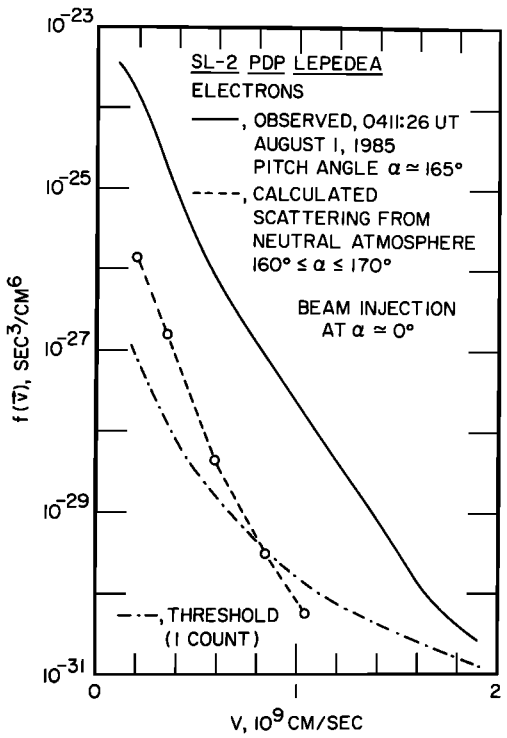


Fig. 2. Electron velocity distribution observed at pitch angle $\alpha \simeq 165°$ in the sheet of returning electrons in the wake of the space shuttle. The velocity distribution expected for secondary electrons from the neutral atmosphere is also shown. The observed upper limit for the velocity distribution just outside the electron sheet is given for comparison.

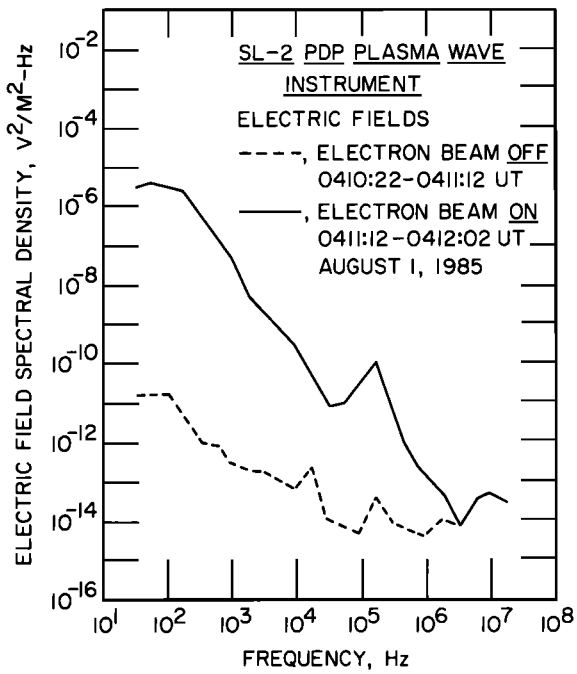


Fig. 3. Electric field spectral densities in the current sheet of returning electrons. Spectral densities for the immediately preceding period when the electron beam is not present are shown for comparison.

The spectral densities of the electric fields increased dramatically in the sheet of returning electrons relative to the densities observed prior to injection of the electron beam. These spectral densities are shown in Figure 3. At 100 Hz the increase is by a factor of $\sim 10^5$ during operation of the electron gun. The local electron plasma frequency, $f_{pe}$, is ~1.3 MHz as determined from measurements of ionospheric densities with a Langmuir probe (courtesy of N. D'Angelo, 1988). Thus the increases of broadband electrostatic noise as shown in Figure 3 occur at frequencies $\lesssim f_{pe}$. Because the electron gyrofrequency $f_c$ is ~0.6 MHz and no well-defined feature of the spectral densities is present at frequencies ~1–2 MHz, the upper frequency cutoff for the broadband electrostatic noise cannot be firmly identified as $f_{pe}$ or the upper hybrid resonance frequency $f_{UHR} = (f_{pe}^2 + f_c^2)^{1/2}$. Simultaneous measurements of the magnetic field spectral densities for the range ~30 Hz to 200 kHz are not available for this crossing of the electron sheet because of the cyclic sampling mode for the search coil which shares the data channel with the electric antenna and Langmuir probe. No increases in magnetic field spectral densities at low frequencies were observed during another, more distant sheet

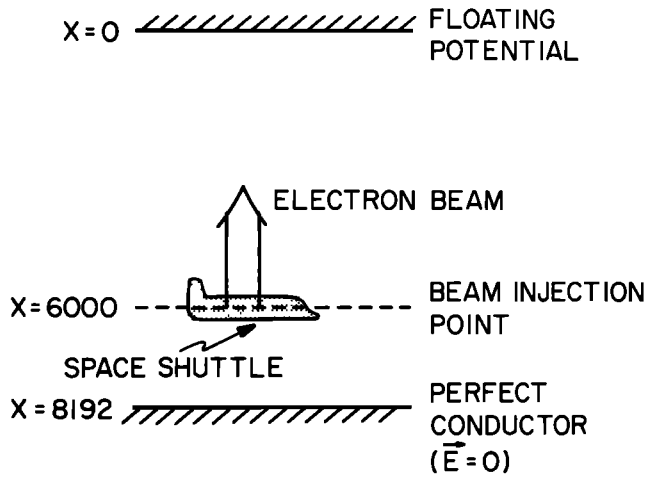


Fig. 4. Geometry assumed for the computer simulation of the injection of the electron beam into the ionosphere with a nonperiodic, one-dimensional electrostatic code.

crossing at 0248 UT. The increases of broadband electrostatic noise were similar to those shown in Figure 3. *Gurnett et al.* [1986] have reported observations of whistler mode radiation from the electron beam during the Spacelab 2 mission as the PDP approached within ~10 m of the magnetic field lines of the electron beam. At these small distances the low-frequency broadband noise is observed in electric and magnetic components, and the relative contributions from electromagnetic and electrostatic modes to the electric field spectral densities cannot be resolved. *Bush et al.* [1987] and *Reeves et al.* [1988*b*] also present observations of the electromagnetic radiation associated with the electron beam during the Spacelab 2 mission. The presence of this whistler mode radiation during the presently discussed observations is identified by the spectral peak at ~200 kHz in Figure 3. This conclusion is based upon the funnel-shaped frequency-time spectrum that is evident in the electric field spectrograms (not shown here).

## Interpretation and Discussion

In order to model electron beam injection into an ambient plasma from the space shuttle for a comparison with observations, a nonperiodic one-dimensional electrostatic particle code is used [*Okuda et al.*, 1987]. The reader is referred to *Birdsall and Langdon* [1985] for a discussion of basic algorithms used in these simulations. As illustrated in Figure 4, the top boundary at $X = 0$ is free whereby plasma crossing the boundary to $X < 0$ is lost from the system and the electric potential can float to any value according to the charge density. The bottom boundary at $X = L = 8192\Delta$ (where $\Delta$ is the grid size, set equal to the electron Debye length $\lambda_e$) is modeled as a perfect conductor with the electric field at $X = L$ set equal to zero, and the plasma particles are reflected with $v \rightarrow -v$ when they reach the bottom boundary. The beam is injected at $X = 6000\Delta$ into a charge neutral background plasma and moves toward $X = 0$ (which is in the negative $x$ direction in simulation coordinates) with a drift speed $V_d = -20v_{te}$. It is assumed that the shuttle injects the beam from a position $X = 6000\Delta$. Thus the boundary at $X = L$ represents the conducting ionosphere, and the PDP which measures the plasma diagnostics (and lags behind the shuttle) would arrive at some position $0 < X < 6000\Delta$ after beam injection, according to the observational geometry of Figure 1.

Because low-frequency ion waves and ion time scales are of interest here, the full dynamics of both ions and electrons must be followed, and a reduced mass ratio $m_i/m_e = 100$ is used. The density of ambient plasma particles $n_0$ is initially 40 per grid space, and the beam density is $n_b = n_0/8$. The ion and electron temperatures are initially equal ($T_e = T_i$). The electron beam temperature $T_b = T_e$. When the beam electrons (injected at $X = 6000\Delta$ with $V_d = -20v_{te}$) reach the top boundary at $X = 0$, the simulation run is stopped.

At $t = 0$, only a charge neutral ambient plasma is present in the system, and for $t > 0$ the introduction of the beam electrons at $X = 6000\Delta$ creates a net negative charge in that region. This charge imbalance creates an electric field in front of the beam, from $X = 0$ to $X = 6000\Delta$, while behind the beam ($6000\Delta < X < L$) the electric field is zero because of the conducting ionosphere at $X = L$. The electric field in front of the beam accelerates the ambient electrons to the top so that, in effect, the injected beam pushes the electrons ahead such that charge neutrality can be maintained in the plasma. The ambient electrons pushed ahead of the beam are lost from the system at $X = 0$, and a rough balance is achieved such that the number of new electrons introduced by beam injection is about equal to the number of ambient electrons that exit the system at the top under the influence of the induced electric field.

The drift of the ambient electrons caused by the induced electric field is not a return current like that found in the beam injection simulations of *Ashour-Abdalla and Okuda* [1986] and *Okuda and Ashour-Abdalla* [1988], because the drifting electrons move away from the spacecraft (and injected beam) rather than back toward it. However, there are

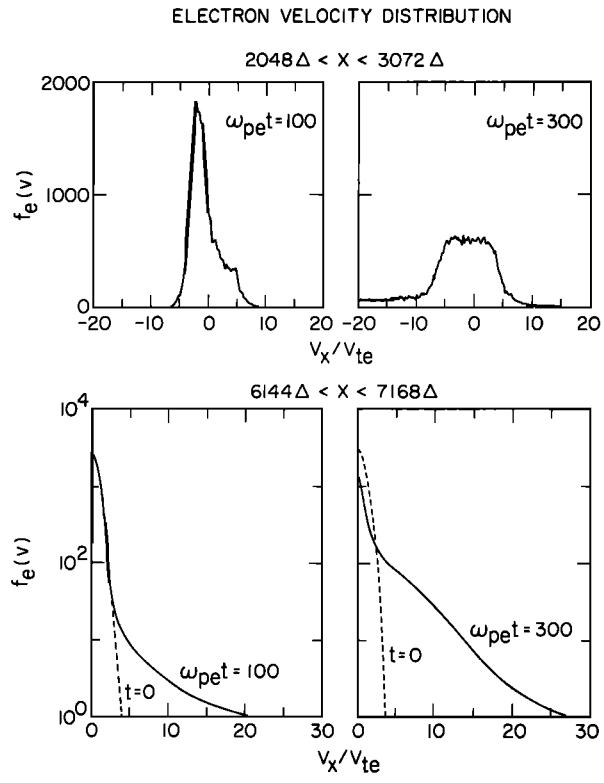


Fig. 5. Temporal evolution of the electron velocity distribution for two different locations in the simulation model shown in Figure 4.

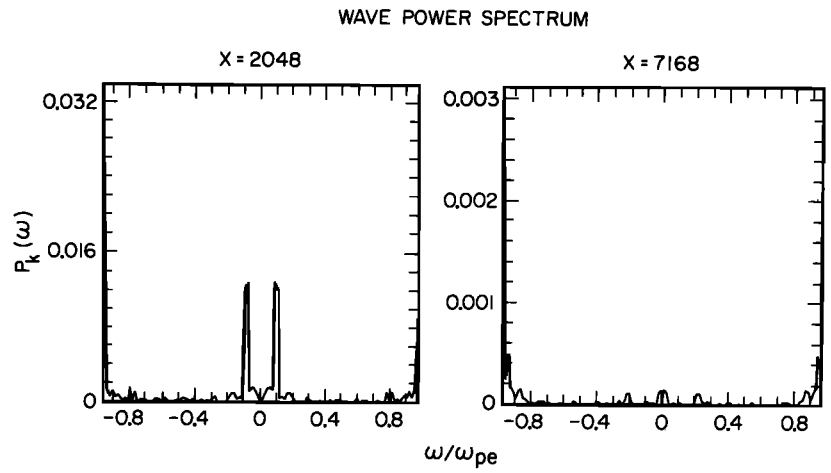


Fig. 6. Computed wave power spectral densities at two locations in the simulation model for $\omega_{pe}t = 300$.

electrons that can be accelerated in the direction opposite to the beam velocity and can be detected by the PDP. This occurs as a result of wave-particle interactions due to plasma instabilities excited by the drifting ambient electrons. The induced electric field caused by the injection of the electron beam at $X = 6000\Delta$ accelerates the ambient electrons at $X < 6000\Delta$ to the top, and the net drift between the ambient ions and drifting ambient electrons can then drive the ion acoustic instability. This process is similar to that described by *Okuda and Ashour-Abdalla* [1988], for which an ion acoustic instability was excited not by the injected beam but by the return current.

The ion acoustic instability is excited by an electron-ion drift [*Fried and Gould*, 1961; *Hasegawa*, 1975] where in the ion rest frame, the ion acoustic phase velocity will occur on the negative slope of the electron velocity distribution function and the instability results from inverse electron Landau damping. The ion acoustic mode propagates parallel to the ambient magnetic field, and for short wavelengths ($k\lambda_e > 1$) the frequency approaches the ion plasma frequency. The velocity threshold at which the instability is excited decreases as $T_e/T_i$ increases greater than 1, but for $T_e = T_i$, the instability can still be unstable for high enough drift velocity [*Gary and Omidi*, 1987]. This critical drift velocity is reached by the ambient electrons in the simulation run, and the ion acoustic instability is excited.

To illustrate how the instability is excited in the simulation run, the electron velocity distribution is shown in Figure 5. The top two panels show the ambient electron velocity distribution at $2048\Delta < X < 3072\Delta$, which is in front of the beam. The top left panel is for $\omega_{pe}t = 100$, and the distribution is seen to be shifted to a negative drift velocity by the induced electric field. The negative slope is unstable to the ion acoustic instability, and the slope already shows plateauing due to quasi-linear diffusion which accelerates the electrons to $v > 0$ and forms a positive velocity high-energy tail. The top right panel shows that at the end of the simulation, when $\omega_{pe}t = 300$, the unstable slope is completely eliminated by diffusion due to the ion acoustic instability and the high-energy tail for $v > 0$ is much more pronounced than at earlier times. These high-energy electrons, accelerated by the wave-particle interactions, flow to the bottom and can penetrate the region behind the beam at $X > 6000\Delta$. This is seen in the bottom two panels of Figure 5, which show (on a semilog plot) the electron velocity distribution at $6144\Delta < X < 7168\Delta$, which is behind the injection of the beam. At $\omega_{pe}t = 100$, shown in the bottom left panel, there is no net drift velocity evident in the velocity distribution, as is expected because the electric field is zero in the region behind the beam. However, a few of the high-energy particles with $v > 0$ created at $X < 6000\Delta$ have already reached this spatial region, and a slight high-energy tail is present. By the end of the simulation, as shown in the bottom right panel, a number of the high-energy electrons have reached $X > 6144\Delta$, and a considerable high-energy tail is formed, similar to that observed with the PDP. Note that the PDP is not located in a position such that the electron plasma oscillations in the beam can be observed, but is positioned behind the electron beam as it propagates along the magnetic field.

An examination of the wave spectrum from the simulation run confirms that ion acoustic waves are excited. Figure 6 shows the wave power spectrum at two different locations along the simulation box. The left panel is taken for $X = 2048\Delta$, which is in front of the beam injection, and two types of waves are excited. At high frequencies near $\omega_{pe}$, plasma oscillations are excited by the injected beam. This excitation is expected because the primary beam is unstable to a Buneman type two-stream instability excited by the relative drift between the injected beam and the ambient plasma background. Lower-frequency waves are also present at just less than $\omega_{pi}$. These ion acoustic waves are excited by the background electron drift as already described. (Note that because of the reduced mass ratio, $\omega_{pi}/\omega_{pe} = (m_e/m_i)^{1/2} = 0.1$.) The observed broadband electrostatic noise spectrum extends to frequencies above $\omega_{pi}$ and could be explained in terms of Doppler shifting of the waves. The right panel shows the power spectrum for $X = 7168\Delta$, which is behind the beam, and it is clear that no ion acoustic waves are excited because there is no drift of the ambient plasma in this region. The ordinate scale is a factor of ~0.1 less than that of the left panel. A weak plasma oscillation is present, but the wave power is nearly an order of magnitude less than that shown in the left panel.

For numerical simulation that is intended to account for observed plasma phenomena it is useful to compare the parameters. The beam density $n_b$ used in the numerical simulation is $n_0/8$, where $n_0$ is the ambient thermal density. The actual electron beam was injected nearly parallel to the

magnetic field. If the range of pitch angles for beam injection is $\alpha \simeq 0°$–$10°$, then the beam density for a homogeneous electron distribution over these pitch angles is about $n_0/2.9$, where $n_0 = 2 \times 10^4$ el/cm$^3$. For the simulation the drift speed $V_d$ for the beam electrons is assumed to be $20v_{te}$, where $v_{te}$ is the characteristic thermal speed of the ambient electrons. A reduced mass ratio $m_i/m_e$ is used. For the injection of the electron beam from the space shuttle, $V_d \simeq 75v_{te}$. The simulation was performed over times extending to about $\omega_{pe}t \simeq 300$. Observations of the electron plasmas and plasma waves with the PDP as reported here occurred at a distance of ~30 m from the space shuttle, or $\omega_{pe}t \simeq 3 \times 10^4$. The PDP is not simultaneously located on the magnetic field line when the electron beam is injected (see Figure 1). For a given field line and pitch angles for electron injection of $0° \lesssim \alpha \lesssim 10°$, the length of the electron column along the field line is ~4 km, i.e., the propagation distance of a 1-keV electron as the shuttle moves a distance across the magnetic field of twice the gyroradius for $\alpha = 10°$. The numerical simulation follows the beam propagation ~0.7 km along the field line. By the time that the field line is intercepted by the PDP the beam electrons have propagated ~70 km from this spacecraft. As shown in Figure 1, the PDP intercepts plasmas along the field line that the beam has previously traversed. The simulation model appears to demonstrate that it is the electron beam and not the return flux of electrons that excites the broadband electrostatic noise. Thus the observed waves may represent only the decaying waves that were previously excited directly in the electron beam. Further numerical simulations, together with observations at various distances in the sheet of returning electrons, are required to resolve this issue. The parameters chosen for the present numerical model are sufficiently similar to the observed plasma parameters that a possible mechanism for beam interaction with the ambient ionosphere can be initially identified and pursued in later studies.

The simulation results can be summarized as follows: (1) the injected electron beam excites plasma oscillations due to the relative beam-background drift and also creates a charge imbalance in the plasma which induces an electric field in front of the beam, (2) the induced electric field forces the background electrons to drift in relation to the background ions, exciting the ion acoustic instability, and (3) the ion acoustic instability, through quasi-linear diffusion, creates an electron high-energy tail in the direction opposite of the injected beam, and these hot electrons are observed by the PDP.

*Acknowledgments.* The authors are grateful to N. D'Angelo for the use of thermal electron plasma measurements from the Langmuir probe. This research was supported in part at The University of Iowa by NASA under contract NAS8-32807 and grants NAG3-449 and NGL-16-001-002, at the University of California, Los Angeles, by the Air Force under contracts F19628-88-K-0011 and F19628-88-K-0022, and at Stanford University and Utah State University by NASA under contract NAS8-36011 and grant NAGW-235. Part of the computing was performed at the San Diego Supercomputer Center supported by the National Science Foundation.

The Editor thanks W. Bernstein and another referee for their assistance in evaluating this paper.

## REFERENCES

Ashour-Abdalla, M., and H. Okuda, Electron acoustic instabilities in the geomagnetic tail, *Geophys. Res. Lett.*, *13*, 366, 1986.

Beghin, C., J. P. Lebreton, B. N. Maehlum, J. Troim, P. Ingsoy, and J. L. Michau, Phenomena induced by charged particle beams, *Science*, *225*, 188, 1984.

Birdsall, C. K., and A. B. Langdon, *Plasma Physics via Computer Simulation*, McGraw-Hill, New York, 1985.

Bush, R. I., G. D. Reeves, P. M. Banks, T. Neubert, P. R. Williamson, W. J. Raitt, and D. A. Gurnett, Electromagnetic fields from pulsed electron beam experiments in space: Spacelab-2 results, *Geophys. Res. Lett.*, *14*, 1015, 1987.

Duprat, G. R. J., B. A. Whalen, and A. G. McNamara, Measurements of the stability of energetic electron beams in the ionosphere, *J. Geophys. Res.*, *88*, 3095, 1983.

Fried, B. D., and R. W. Gould, Longitudinal ion oscillations in a hot plasma, *Phys. Fluids*, *4*, 139, 1961.

Gary, S. P., and N. Omidi, The ion-ion acoustic instability, *J. Plasma Phys.*, *37*, 45, 1987.

Grandal, B. (Ed.), *Artificial Particle Beams in Space Plasma Studies*, Plenum, New York, 1982.

Gurnett, D. A., W. S. Kurth, J. T. Steinberg, P. M. Banks, R. I. Bush, and W. J. Raitt, Whistler-mode radiation from the Spacelab 2 electron beam, *Geophys. Res. Lett.*, *13*, 225, 1986.

Hasegawa, A., Plasma instabilities and nonlinear effects, in *Physics and Chemistry in Space*, vol. 8, edited by J. Roederer and J. T. Wasson, p. 17, Springer-Verlag, New York, 1975.

Hedin, A. E., A revised thermospheric model based on mass spectrometer and incoherent scatter data: MSIS-83, *J. Geophys. Res.*, *88*, 10,170, 1983.

Hess, W. N., M. C. Trichel, T. N. Davis, W. C. Beggs, G. E. Kraft, E. Stassinopoulos, and E. J. R. Maier, Artificial auroral experiment: Experiment and principal results, *J. Geophys. Res.*, *76*, 6067, 1971.

Maehlum, B. N., B. Grandal, T. A. Jacobsen, and J. Troim, Polar 5—An electron accelerator experiment within an aurora, 2, Scattering of an artificially produced electron beam in the atmosphere, *Planet. Space Sci.*, *28*, 279, 1980.

Okuda, H., and M. Ashour-Abdalla, Ion acoustic instabilities excited by injection of an electron beam in space, *J. Geophys. Res.*, *93*, 2011, 1988.

Okuda, H., R. Horton, M. Ono, and M. Ashour-Abdalla, Propagation of a nonrelativistic electron beam in a plasma in a magnetic field, *Phys. Fluids*, *30*, 200, 1987.

Opal, C. B., W. K. Peterson, and E. C. Beaty, Measurements of secondary-electron spectra produced by electron impact ionization of a number of simple gases, *J. Chem. Phys.*, *55*, 4100, 1971.

Raitt, W. J., P. M. Banks, W. F. Denig, and H. R. Anderson, Transient effects in beam-plasma interactions in a space simulation chamber stimulated by a fast pulse electron gun, in *Artificial Particle Beams in Space Plasma Studies*, edited by B. Grandal, p. 405, Plenum, New York, 1982.

Reeves, G. D., P. M. Banks, A. C. Fraser-Smith, T. Neubert, R. I. Bush, D. A. Gurnett, and W. J. Raitt, VLF wave stimulation by pulsed electron beams injected from the space shuttle, *J. Geophys. Res.*, *93*, 162, 1988*a*.

Reeves, G. D., P. M. Banks, T. Neubert, R. I. Bush, P. R. Williamson, A. C. Fraser-Smith, D. A. Gurnett, and W. J. Raitt, VLF wave emissions by pulsed and DC electron beams in space, 1, Spacelab 2 observations, *J. Geophys. Res.*, *93*, 14,699, 1988*b*.

Shawhan, S. D., Description of the plasma diagnostics package (PDP) for the OSS-1 shuttle mission and JSC plasma chamber test in conjunction with the fast pulse electron gun (FPEG), in *Artificial Particle Beams in Space Plasma Studies*, edited by B. Grandal, p. 419, Plenum, New York, 1982.

Wilhelm, K., W. Studemann, and W. Riedler, Electron flux intensity distributions observed in response to particle beam emissions, *Science*, *225*, 186, 1984.

Wilhelm, K., W. Bernstein, P. J. Kellogg, and B. A. Whalen, Fast magnetospheric echoes of energetic electron beams, *J. Geophys. Res.*, *90*, 491, 1985.

Winckler, J. R., The application of artificial electron beams to magnetospheric research, *Rev. Geophys.*, *18*, 659, 1980.

Winckler, J. R., R. L. Arnoldy, and R. A. Hendrickson, Echo 2: A study of electron beams injected into the high-latitude ionosphere from a large sounding rocket, *J. Geophys. Res.*, *80*, 2083, 1975.

Winglee, R. M., and P. L. Pritchett, Comparative study of cross-field and field-aligned electron beams in active experiments, *J. Geophys. Res.*, *93*, 5823, 1988.

M. Ashour-Abdalla and N. Omidi, Institute of Geophysics and Planetary Physics, University of California, Los Angeles, CA 90024.
P. M. Banks and R. I. Bush, STAR Laboratory, Stanford University, Stanford, CA 94305.
L. A. Frank, D. A. Gurnett, W. S. Kurth, and W. R. Paterson, Department of Physics and Astronomy, University of Iowa, Iowa City, IA 52242.
W. J. Raitt, CASS, Utah State University, Logan, UT 84322.
D. Schriver, Max-Planck-Institut für Extraterrestrische Physik, 8046 Garching, Federal Republic of Germany.

(Received January 3, 1989;
revised February 16, 1989;
accepted March 8, 1989.)